

PAPER • OPEN ACCESS

Influence of Coulomb disorder on the phase diagrams of the Anderson-Hubbard model

To cite this article: Nguyen Thi Hai Yen *et al* 2022 *J. Phys.: Conf. Ser.* **2269** 012004

View the [article online](#) for updates and enhancements.

You may also like

- [Phase diagram of the anisotropic Anderson transition with the atomic kicked rotor: theory and experiment](#)
Matthias Lopez, Jean-François Clément, Gabriel Lemarié et al.
- [Anderson transition on the Bethe lattice: an approach with real energies](#)
Giorgio Parisi, Saverio Pascazio, Francesca Pietracaprina et al.
- [Multitude of phases in correlated lattice fermion systems with spin-dependent disorder](#)
J Skolimowski, D Vollhardt and K Byczuk

Influence of Coulomb disorder on the phase diagrams of the Anderson-Hubbard model

Nguyen Thi Hai Yen^{1,2}, Hoang Anh Tuan^{1,2}, Le Duc Anh³

¹ Institute of Physics, Vietnam Academy of Science and Technology, Vietnam

² Graduate University of Science, Vietnam Academy of Science and Technology, Vietnam

³ Faculty of Physics, Hanoi National University of Education, Vietnam

E-mail: hatuan@iop.vast.ac.vn, hatuan@iop.vast.vn

Abstract. We study the half-filled Hubbard model with Anderson and Coulomb disorder by mean of dynamical mean field theory using the geometrically averaged local density of states. The paramagnetic phase diagram of the model as a function of the Coulomb interaction and Anderson disorder strength is obtained. The spectral phase diagrams of the ground states for the model are also constructed and discussed. We show that in the intermediate and strong interaction regimes, the Coulomb disorder leads the metallic and Mott insulator phase regions shrink, while the Anderson insulator region is enlarged.

1. Introduction

The metal - insulator transitions (MITs) are one of the most interesting problems in condensed matter physics for both theoretical and experimental research. This phenomenon usually occurs at a low temperature, and the MITs are at zero temperature $T = 0$ which is the quantum transition. The critical points obtained here are called the quantum critical. The metallic and insulator phase are distinguished from each other by an order parameter at critical points [1]. In addition, the Mott insulator [2] (caused by Coulomb interaction) responds to the local density of states (LDOS) that have a gap at the Fermi level, no gap for the metallic phase, and change from continuing to discrete and lie dense value for the Anderson localization [3] (caused by disorder).

In a disordered system, the probability distribution function of random variables is not completely known. The first moment (the mean value) is not enough to describe the properties of these variables and the typical value (the value has the maximum probability) is most important in this situation. In 2003, Dobrosaljvec proposed the approximation that the geometrically averaged LDOS may be set to equal the typical medium value of LDOS [4]. The geometrically averaged LDOS is vanished while the arithmetically averaged one is still finite at the critical point of the Anderson localization. This theory has proven effective to describe the Anderson localization [5, 6, 7, 8, 9].

To study systems with both disorder and interaction, there are two famous models, which are Anderson - Hubbard model (AHM) and Anderson - Falikov - Kimball model (AFKM). The interplay between Anderson structural disorder and an arbitrary Coulomb interaction value in the AHM model leads to a nonmagnetic phase diagram consisting of three phases: correlated metal, Mott insulator, and Anderson localization [8, 9]. In addition, the phase diagrams for AFKM was built when both Anderson disorder and Coulomb interaction disorder were present



[6, 7]. The results show that the metallic and the Mott insulator phase regions are narrowed, and the Anderson insulator region is enlarged when the Coulomb disorder strength increases. This means that the role of Coulomb disorder cannot be ignored when considering the system with interaction and disorder. In the following, we study the influence of Coulomb disorder on the phase diagrams of the ground states for the AHM and compare them to those of the AFKM.

The models of disordered and interacting fermion systems have been realized in experiments on an optical lattice [10, 11, 12, 13]. These are very important steps forward in testing our understanding of quantum phase transitions. The investigations in ultracold atoms have numerous advantages, i.e., the optical potential for atoms can be controlled and varied by the light intensities or frequencies, and interaction strength can be changed by Feshbach resonances. These experiments can be expected to become very active in a near future to understand the MITs in the strongly interacting and disordered fermion systems.

The paper is organized as follows. In Section 2 we present the model and method for the fermionic system that has both Anderson structural and Coulomb interaction disorder. The equation of motion method is used as the impurity solver within the dynamical mean field theory (DMFT), and the typical medium value of the LDOS is approximated by the geometrically averaged LDOS. In Section 3, the nonmagnetic phase diagram of the model is obtained from the geometrically and arithmetically averaged LDOS. In addition, the spectral phase diagrams is also constructed and discussed. The conclusions are given in the Section 4.

2. Model and formalism

We focus on the Anderson - Hubbard model, as defined by the following Hamiltonian

$$H = -t \sum_{\langle ij \rangle \sigma} (a_{i\sigma}^\dagger a_{j\sigma} + \text{H.c.}) + \sum_{i\sigma} (\varepsilon_i - \mu) n_{i\sigma} + \sum_i U_i [n_{i\uparrow} n_{i\downarrow} - \frac{1}{2}(n_{i\uparrow} + n_{i\downarrow})], \quad (1)$$

where $a_{i\sigma}^\dagger$ ($a_{i\sigma}$) is the creation (annihilation) operator of an electron at site i with spin σ , t is the hopping amplitude between nearest neighbor sites i and j . The on-site Coulomb interaction U_i and the local impurities ε_i are random variables. We assume a box distribution for both ε_i and U_i : $P(\varepsilon_i) = \theta(\delta/2 - |\varepsilon_i|)/\Delta$ and $\tilde{P} = \theta(\delta/2 - |U_i - U|)/\delta$, respectively, where θ is the step function. $\Delta(\delta)$ measures the strength of structural Anderson (Coulomb) disorder, and U is the mean value of the Coulomb interaction strength. Here, we deal only with the repulsive interaction, $U_i \geq 0$, which leads to $U \geq \delta/2$.

The Hamiltonian model (1) is solved via typical medium theory with an approximation to the equation of motions. In the result the impurity Green function $G(\omega, \varepsilon_i, U_i)$ can be obtained from decoupling the equations of motion at the second order. Then the local density of states is given by

$$\rho_i(\omega) = -\frac{1}{\pi} \text{Im} G(\omega, \varepsilon_i, U_i), \quad (2)$$

which depends on ε_i and U_i . In the typical medium theory, the typical LDOS can be approximately replaced by the geometrically averaged LDOS

$$\rho_{geom}(\omega) = \exp \left[\int du \int d\varepsilon P(\varepsilon) \tilde{P}(u) \ln \rho(\omega, \varepsilon, u) \right]. \quad (3)$$

The arithmetically averaged LDOS is also obtained

$$\rho_{arith}(\omega) = \int du \int d\varepsilon P(\varepsilon) \tilde{P}(u) \rho(\omega, \varepsilon, u). \quad (4)$$

The typical Green function is given by the Hilbert transform

$$G_{typ}(\omega) = \int d\omega' \frac{\rho_{geom}(\omega')}{\omega - \omega'}. \quad (5)$$

The lattice Green function can be calculated from the self-energy of the effective medium $\Sigma(\omega)$ and the non-interacting density of states $\rho_0(\omega)$

$$G(\omega) = \int d\omega' \frac{\rho_0(\omega')}{\omega - \Sigma(\omega) - \omega'}. \quad (6)$$

The self-energy $\Sigma(\omega)$ of the effective medium can be determined from Dyson equation

$$\Sigma(\omega) = \omega + \mu - \eta(\omega) - \frac{1}{G(\omega)}, \quad (7)$$

where $\eta(\omega)$ is the hybridization function. We choose the non-interaction density of states $\rho_0(\varepsilon) = 4\sqrt{1 - 4(\varepsilon/W)^2}/(\pi W)$ with bandwidth W , for which the hybridization function is given by

$$\eta(\omega) = \frac{W^2}{16} G(\omega). \quad (8)$$

The self-consistent DMFT equations are closed as follows

$$G(\omega) = G_{typ}(\omega). \quad (9)$$

In this paper, we study the paramagnetic and half-filling case, i.e., $\langle n_i \uparrow \rangle = \langle n_i \downarrow \rangle = \langle n_i \rangle / 2$ and $\mu = 0$. In this case, the ground state can be determined from the averaged LDOS at the Fermi level: nonzero value of $\rho_{geom}(0)$ denotes a metallic phase; $\rho_{arith}(0) = 0$ indicates a Mott insulator phase (hard gap); and an Anderson insulator phase (gapless) is signaled by $\rho_{geom}(0) = 0$, $\rho_{arith}(0) > 0$. For simplicity of calculation, we use the atomic limit for $\langle n_i \rangle$.

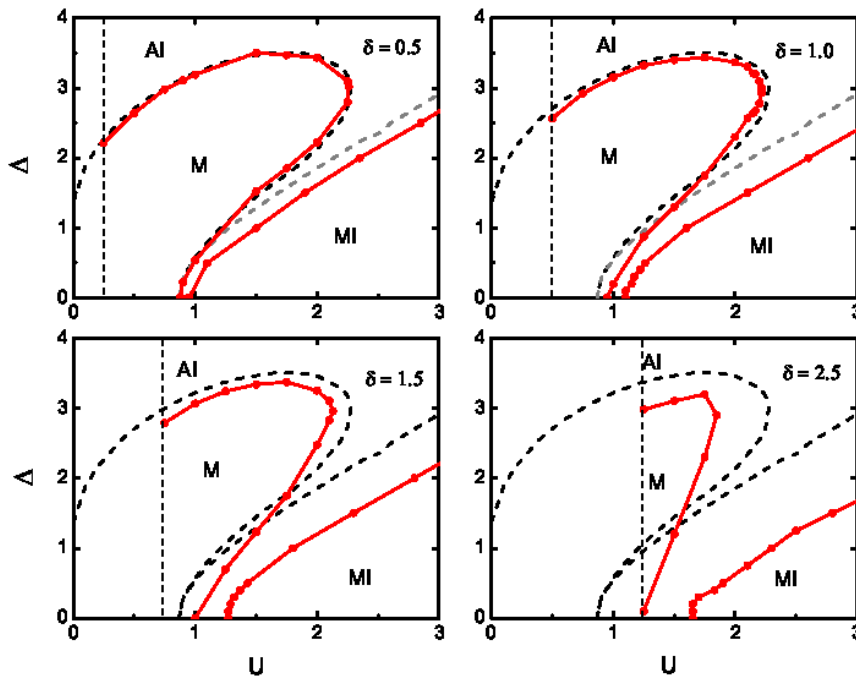


Figure 1. Phase diagrams of the AHM for different Coulomb disorder strengths (solid red lines) compared with to those with $\delta = 0$ (dash back lines). The vertical dotted line splits the regions for which $U < \delta/2$ (left side; not considered) and $U \geq \delta/2$ (right side). W sets the energy unit.

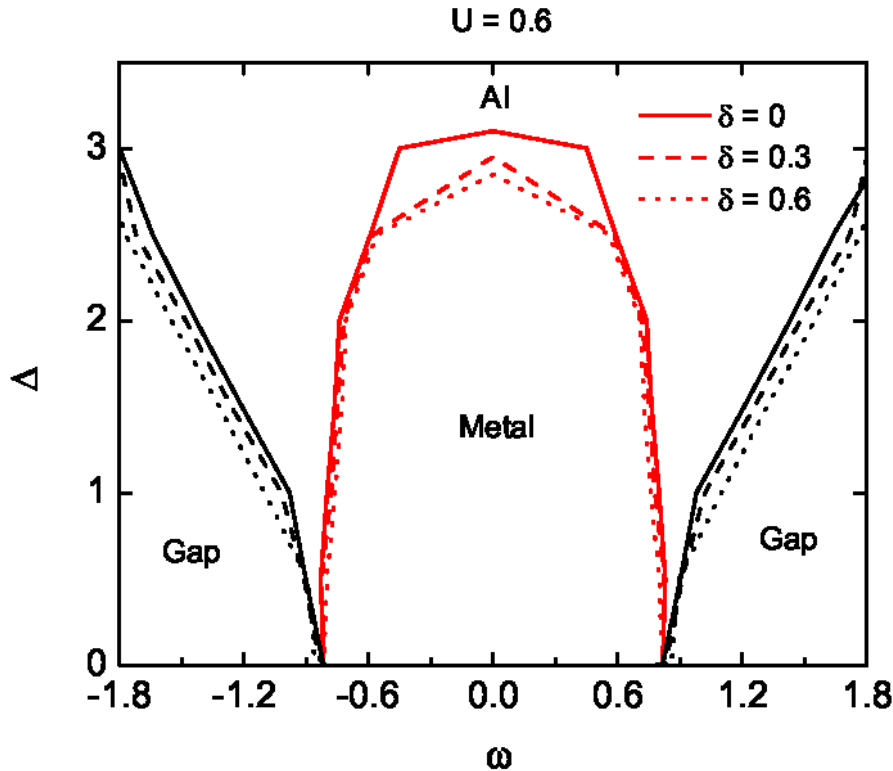


Figure 2. Spectral phase diagram of the ground state for the weak interaction regime ($U = 0.6$) and different Coulomb disorder strengths. Mobility edges (band edges) determined within DMFT with geometric (arithmetic) averaging.

3. Results and Discussion

Now we study the system's phase diagrams obtained from the typical medium theory described in Section 2. To perform the Hilbert transform the fast Fourier transform methods are used. Through this work we set $W = 1$.

The $U - \Delta$ ground state phase diagram of the AHM with different Coulomb disorder strengths ($\delta = 0.5, 1.0, 1.5, 2.5$) (solid red lines) is shown in Fig. 1. We compare them with those of the model without Coulomb disorder ($\delta = 0$) (dash black lines). All the critical curves presented here were obtained by solving the DMFT self-consistent equations (2) - (9) in the band center ($\omega = 0$). It is well known that in the case $\delta = 0$, there are three phases can be found: the correlated metal (M) occurs at small values of both U and Δ , the Anderson insulator (AI) overcomes for large Δ , and the Mott insulator (MI) stabilizes with increasing U [8, 9]. In addition, we found three different interaction regimes regarding the metallic and Mott phase boundaries [9]: weak ($0 < U < \sqrt{3}/2$), intermediate ($\sqrt{3}/2 < U < 2.3$), and strong ($U \geq 2.3$). For the model with Coulomb disorder ($\delta \neq 0$), we only deal with the repulsive Coulomb $U \geq \delta/2$, meaning the values of U is in the right of the vertical dotted line in Fig. 1. With increasing Coulomb disorder, these three regimes still hold but for different critical values and the metallic as well as Mott insulator phase regions shrink, while the Anderson insulator region is enlarged. We note that even in the absence of structural disorder $\Delta = 0$, the presence of Coulomb disorder gives rise to an Anderson localized states.

Next, we construct the spectral phase diagrams on the $\omega - \Delta$ plane. For fixed values of both δ and Δ , the trajectories of mobile edges (red line) and of the band edges (black line) can be obtained by determining the values of frequency ω that averaged LDOS $\rho_{geom}(\omega)$ and $\rho_{arith}(\omega)$

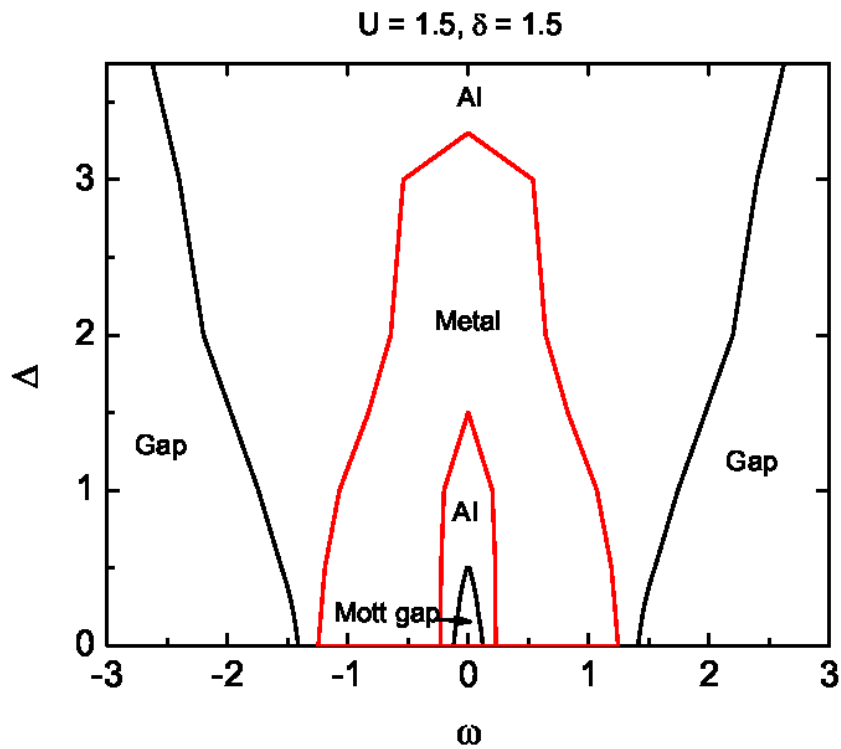


Figure 3. Same as Fig. 2 but for the intermediate interaction regime ($U = 1.5$ and $\delta = 1.5$)

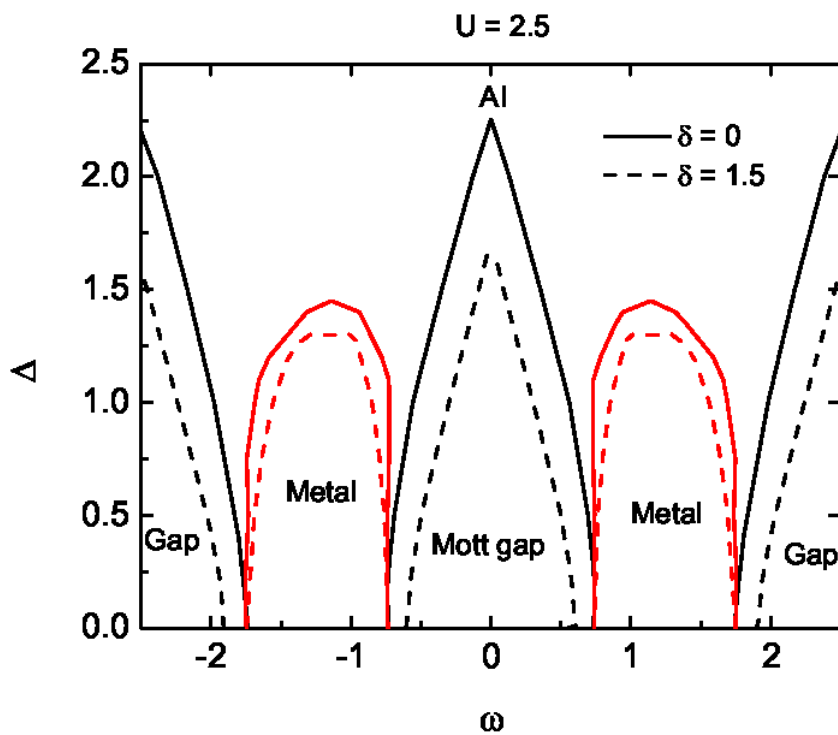


Figure 4. Same as Fig. 2 but for the strong interaction regime ($U = 2.5$ and $\delta = 0, 1.5$).

vanish, respectively. In Fig. 2, the spectral phase diagram in the weak regime of Coulomb interaction ($U = 0.6$) is presented. There is not a Mott gap in the phase diagram and this is qualitatively similar to those obtained for the Anderson model [4] as well as for the Anderson-Falicov - Kimball model [6, 7]. In this case the Coulomb disorder does not significantly effect the system's properties. In Fig. 3, we plot the spectral phase diagram in the intermediate interaction regime. In the present case, a Mott gap is opened around the band center and is surrounded by the Anderson insulator region. As δ increases, the localization rises and the Mott gap vanishes. In addition, the metallic states are bounded between two separated Anderson localized states regions. Finally, the spectral phase diagram for the strong interaction regime is shown in Fig. 4. The spectrum of metallic states is found in two separate lobes. When δ increases, both Mott gap and metallic regions shrink and the surrounded Anderson insulator region is enlarged. We again remark that these results for AHM are qualitatively similar to those obtained for the Anderson-Falicov - Kimball model [6], but they are quantitatively different.

4. Conclusions

In this paper, we construct for the first time the nonmagnetic phase diagram $U - \Delta$ and the spectral phase diagrams $\omega - \Delta$ of the Anderson-Hubbard model with both Anderson structural and Coulomb disorder. We show that in the intermediate and strong interaction regimes, the Coulomb disorder leads the metallic and Mott insulator phase regions shrink, and the Anderson insulator region is enlarged. The Anderson localized states appears even in the absence of Anderson disorder ($\Delta = 0$) if the Coulomb disorder strength is large enough. We also show that the phase diagrams of the AHM with Coulomb disorder are qualitatively similar to those obtained for the AFKM with Coulomb disorder.

Acknowledgments

This work is supported by Vietnam Academy of Science and Technology under Program NVCC05.11/21-21.

References

- [1] Belitz D and Kirkpatrick T R 1994 *Rev. Mod. Phys.* **66** 261.
- [2] Mott N F 1949 *Proc. Phys. Soc. Lond. A* **62** 416.
- [3] Anderson P W 1958 *Phys. Rev.* **109** 1492.
- [4] Dobrosavljevic V, Pastor A A , Nikolic B K 2003 *Europhys. Lett.* **62** 76.
- [5] Byczuk K 2005 *Phys. Rev. B* **71** 205105.
- [6] Carvalho R D B, Almeida G M A, and Souza A M C 2014 *Eur. Phys. J. B* **87** 160.
- [7] Nguyen Thi Hai Yen, Hoang Anh Tuan 2021 *J. Phys.: Conf. Ser.* **1932** 012013.
- [8] Byczuk K, Hofstetter W, and Vollhardt D 2010 *Int. J. Mod. Phys. B* **24** 1727.
- [9] Hoang A T, Nguyen T H Y, Le D A 2019 *Phys. B: Cond Matt.* **570** 320.
- [10] White M, Pasienski M, McKay D, Zhou S Q, Ceperley D, and DeMarco B 2009 *Phys. Rev. Lett.* **102** 055301.
- [11] Deissler B, Zaccanti M, Roati G, D'Errico C, Fattori M, Modugno M, Modugno G, and Inguscio M 2010 *Nature Phys.* **6** 354.
- [12] Deissler B, Lucioni E, Modugno M, Roati G, Tanzi L, Zaccanti M, Inguscio M, and Modugno G 2011 *New J. Phys.* **13** 023020.
- [13] Lucioni E, Deissler B, Tanzi L, Roati G, Zaccanti M, Modugno M, Larcher M, Dalfovo F, Inguscio M, and Modugno G 2011 *Phys. Rev. Lett.* **106** 230403.